A Density Functional Study on the Activation of Hydrogen-Hydrogen and Hydrogen-Carbon Bonds by Cp_2Sc-H and Cp_2Sc-CH_3

T. Ziegler,* E. Folga, and A. Berces

Contribution from the Department of Chemistry, University of Calgary, Calgary, Alberta, Canada T2N 1N4. *Received April 27, 1992*

Abstract: Density functional calculations have been carried out on Cp_2Sc-R (R = H, methyl, ethyl, propyl, vinyl, and acetylide). Geometry optimizations reveal an agostic interaction for R = ethyl, whereas methyl and propyl are bound to the metal center without agostic interactions. The Sc-R bond energies are calculated as D_e(Sc-acetylide) = 540 kJ mol^{-1} > D_e(Sc-H) = 340 > D_e(Sc-vinyl) = 338 > D_e(Sc-methyl) = 295 > D_e(Sc-ethyl) = 283 > D_e(Sc-propyl) = 240. A study on the σ-bond metathesis reaction (I) ($Cp_2Sc-R + H-R' \rightarrow Cp_2Sc-R' + H-R$) reveals the following reaction enthalpies [ΔH_1(R,R'), in kJ mol^{-1}]: ΔH_1(CH_3, acetylide) = −128 < ΔH_1(H, acetylide) = −86 < ΔH_1(CH_3, H) = −28 < ΔH_1(CH_3), vinyl) = −26 < ΔH_1(H, vinyl) = 16. Reaction I proceeds from an adduct (a) between Cp_2Sc-R and H-R' over a kite-shaped four-center transition state (b) with a Sc-R-H-R' core to an adduct (c) between Cp_2Sc-R and H-R'. The activation energies, $\Delta H^{\ddagger}_1$(R,R'), are calculated in kJ mol^{-1} as $\Delta H^{\ddagger}mo_1$(H, acetylide) = −29 < $\Delta H^{\ddagger}_1$(H, H) = −7 < $\Delta H^{\ddagger}_1$(CH_3, acetylide) = −4 < $\Delta H^{\ddagger}_1$(CH_3, H) = 8 < $\Delta H^{\ddagger}_1$(H, vinyl) = 14 < $\Delta H^{\ddagger}_1$(CH_3, vinyl) = 39 < $\Delta H^{\ddagger}_1$(CH_3, CH_3) = 45. The activation energies increase with the number of vinyl and methyl groups in the Sc-R-H-R' core as the directional σ-orbitals on these groups are unable to maintain optimal interactions with both neighbors in the Sc-R-H-R' core. The transition states for reactions with negative activation energies are below the reactants in energy but still above the adduct (a). The formally forbidden [$2_\sigma + 2_\sigma$] reaction is facilitated by a pool of s-, p-, and d-type orbitals on scandium which maintain optimal interactions with the neighboring groups throughout the reaction.

I. Introduction

The ability of metal centers to mediate the breaking and formation of H-H and C-H bonds is of considerable practical importance. Thus, several experimental[1-4] and theoretical[5-9] studies have been undertaken in order to understand these pivotal elementary steps. The initial investigations focused on electron-rich middle to late transition metal centers which can activate (break) H-H[1,5] and C-H[2,5i-k,6a-c] bonds by oxidative addition and subsequently generate new H-H and C-H bonds by reductive elimination. Of crucial importance in these types of reactions is the ability of the metal center to change its formal oxidation state. More recent studies have been directed toward the ability of early electron-poor metal centers to break and form H-H and C-H σ bonds through the σ-bond metathesis-like reaction[3]

$$L_nM\text{-}R^* + H\text{-}R \rightarrow L_nM\text{-}R + H\text{-}R^* \quad (1)$$

($M = d^0, f^{14}d^0$; R* = H, alkyl; R = H, alkyl, alkenyl, alkynyl)

where the formal oxidation state and electron count on the metal center remain unchanged.

The σ-bond metathesis[3h] by organo-lutetium and organo-scandium methyl complexes have been studied experimentally by Watson[3c-e] and Bercaw[3a-b] in connection with the Ziegler-Natta polymerization process. Electron-poor early f-block elements are also known[3f,g] to activate H-H and C-H bonds according to the reaction give in eq 1.

Activation of the H-H and C-H bonds by electron-poor metal centers in the σ-bond metathesis reaction of eq 2 have been

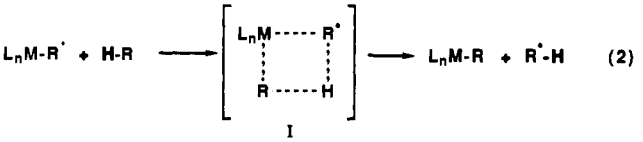

(2)

I

postulated[3] to proceed via a four-center transition state I. Activation of H-H bonds via the four-center transition state I might also occur in complexes of middle to late transition metals.[9]

Up-to-date theoretical investigations on σ-bond metathesis include a GVB (generalized valence bond) study of the reaction in eq 1 (M = Sc, Ti; L = Cl) with R* = H, R = H by Goddard and Steigerwald[7a] and EHA (extended Hückel approximation) calculations of the reaction in eq 1 (M = Lu; L = Cp*) with R* = H, R = H and R* = CH_3, R = CH_3 by Hoffmann and coworkers.[7c] Recently, Rappé[7b] has discussed σ-bond metathesis

(1) Kubas, G. J. *Acc. Chem. Res.* **1988**, *21*, 120.
(2) (a) Janowicz, A. H.; Bergman, R. G. *J. Am. Chem. Soc.* **1982**, *104*, 352. (b) Hoyano, J. K.; Graham. W. A. G. *J. Am. Chem. Soc.* **1982**, *104*, 3723. (c) Jones, W. D.; Feher, F. J. *J. Am. Chem. Soc.* **1984**, *106*, 1650. (d) Jones, W. D.; Feher, F. J. *Acc. Chem. Res.* **1989**, *22*, 91. (e) Rothwell, I. P. *Acc. Chem. Res.* **1988**, *21*, 153. (f) Crabtree, R. H. *Chem. Rev.* **1985**, *85*, 245. (g) Martinho Simoes, J. A.; Beauchamp, J. L. *Chem. Rev.* **1990**, *90*, 629.
(3) (a) Burger, B. J.; Thompson, M. E.; Cotter, W. D.; Bercaw, J. E. *J. Am. Chem. Soc.* **1990**, *112*, 1566. (b) Thompson, M. E.; Buxter, S. M.; Bulls, A. R.; Burger, B. J.; Nolan, M. C.; Santarsiero, B. D.; Schaefer, W. P.; Bercaw, J. E. *J. Am. Chem. Soc.* **1987**, *109*, 203. (c) Watson, P. L. *J. Chem. Soc., Chem. Commun.* **1983**, 276. (d) Watson, P. L.; Parshall, G. W. *Acc. Chem. Res.* **1985**, *18*, 51. (e) Watson, P. L. *J. Am. Chem. Soc.* **1983**, *105*, 6491. (f) Jeske, G.; Lauke, H.; Mauermann, H.; Schumann, H.; Marks, T. J. *J. Am. Chem. Soc.* **1985**, *107*, 8111. (g) Bruno, J. W.; Smith, G. M.; Marks, T. J.; Fair, C. K.; Shultz, A. T.; Williams, J. M. *J. Am. Chem. Soc.* **1986**, *108*, 40. (h) Davis, J. A., Watson, P. L., Liebman, J. F., Greenberg, A., Eds.; *Selective Hydrocarbon Activation*; VCH Publishers: New York, 1990. (i) McDade, C.; Bercaw, J. E. *J. Organomet. Chem.* **1985**, *279*, 281.
(4) (a) Christ, C. S., Jr.; Eyler, J. R.; Richardson, D. E. *J. Am. Chem. Soc.* **1990**, *112*, 596. (b) Christ, C. S., Jr.; Eyler, J. R.; Richardson, D. E. *J. Am. Chem. Soc.* **1988**, *110*, 4038.
(5) (a) Kitaura, K.; Obara, S.; Morokuma, K. *J. Am. Chem. Soc.* **1981**, *103*, 2891. (b) Obara, S.; Kitaura, K.; Morokuma, K. *J. Am. Chem. Soc.* **1984**, *106*, 7482. (c) Noell, J. O.; Hay, P. J. *J. Am. Chem. Soc.* **1982**, *104*, 4578. (d) Low, J. J.; Goddard, W. A. *J. Am. Chem. Soc.* **1984**, *106*, 6928. (e) Blomberg, M. R. A.; Siegbahn, P. E. M. *J. Chem. Phys.* **1983**, *78*, 986. (f) Blomberg, M. R. A.; Siegbahn, P. E. M. *J. Chem. Phys.* **1983**, *78*, 5682. (g) Brandemark, U. B.; Blomberg, M. R. A.; Pettersson, L. G. M.; Siegbahn, P. E. M. *J. Phys. Chem.* **1984**, *88*, 4617. (h) Low, J. J.; Goddard, W. A. *J. Am. Chem. Soc.* **1984**, *106*, 8321. (i) Low, J. J.; Goddard, W. A. *Organometallics* **1986**, *5*, 609. (k) Low, J. J.; Goddard, W. A. *J. Am. Chem. Soc.* **1986**, *108*, 6115. (l) Saillard, J-Y.; Hoffmann, R. *J. Am. Chem. Soc.* **1984**, *106*, 2006.
(6) (a) Hofmann, P.; Padmanabhan, M. *Organometallics* **1983**, *2*, 1273. (b) Dedieu, A. In *Topics in Physical Organometallic Chemistry*; Gielen, M. F., Ed.; Freund Publishing House: London, 1989; Vol. 1, p 1. (c) Ziegler, T.; Fan, L.; Tschinke, V.; Becke, A. *J. Am. Chem. Soc.* **1989**, *111*, 2018. (d) Ziegler, T.; Tschinke, V.; Becke, A. *J. Am. Chem. Soc.* **1987**, *109*, 1351. (e) Ziegler, T.; Wendan, C.; Baerends, E. J.; Rawenek, W. *Inorg. Chem.* **1988**, *27*, 3458. (f) Ziegler, T.; Tschinke, V.; Versluis, L.; Baerends, E. J. *Polyhedron* **1988**, *7*, 1625.
(7) (a) Steigerwald, M. L.; Goddard, W. A., III *J. Am. Chem. Soc.* **1984**, *106*, 308. (b) Rappé, A. K. *Organometallics* **1990**, *9*, 466. (c) Rabaâ, H.; Sailard, J.-Y.; Hoffmann, R. *J. Am. Chem. Soc.* **1986**, *108*, 4327. (d) Folga, E.; Ziegler, T. *New. J. Chem.* **1991**, *15*, 741. (e) Folga, E.; Ziegler, T. *Can. J. Chem.* **1992**, *70*, 333.
(8) Jolly, C. A.; Marynick, D. S. *J. Am. Chem. Soc.* **1989**, *111*, 7968.
(9) Versluis, L.; Ziegler, T. *Organometallics* **1990**, *9*, 2985.

0002-7863/93/1515-636$04.00/0

between C–H bonds of acetylenes and the Cl_2Sc-R (R = H, CH_3) linkage. We[7d,e] have also reported preliminary calculations on the reaction in eq 1 with ML_n = $LuCl_2$ and R* = H, CH_3; R = H, CH_3.

The present investigation is concerned with Cp_2Sc-R (R = H, alkyl, alkenyl, and alkynyl) as well as the ability of Cp_2Sc-H and Cp_2Sc-CH_3 to undergo σ-bond metathesis reactions with C–H bonds of methane, ethylene, and acetylene.

The structural details of the Sc–R linkage are of considerable interest,[3b] in particular with regard to a possible agostic interaction between the electropositive metal center and C–H bonds on R. Until now only $Cp^*_2Sc-CH_3$ has been studied by diffraction methods;[3b] however, this study did not allow for a location of the methyl hydrogens. Various spectroscopic techniques[3b] have been applied to other Sc–R systems, but conclusive evidence for an agostic interaction has been elusive. We shall present optimized structures for R = methyl, ethyl, and propyl as well as R = vinyl and acetylide. Closely related to the agostic C–H interaction is the migration of hydride from R to the metal center. This migration, which ultimately leads to a decomposition of the Sc–R bond, will also be investigated. We shall, in addition, study the strength of the Sc–R linkage and compare it to the corresponding H–R bond.

The second part of our investigation is concerned with the σ-bond metathesis reaction of eq 2 and the structure of the related transition state I. We shall examine the factors which enable this formally forbidden $[2_\sigma + 2_\sigma]$ addition reaction to proceed in contrast to the $[2_\sigma + 2_\sigma]$ addition between H–H and C–H σ-bonds which is associated with an insurmountable barrier. Attention will also be given to possible intermediates along the reaction path and to the different roles played by the Sc–H and Sc–CH_3 bonds in the reaction. Experiments have clearly demonstrated that the alkynylic C–H bonds undergo the metathesis reaction of eq 1 much more readily than alkylic C–H bonds in spite of the fact that the former type of bonds is much stronger than the latter. We shall compare the ease by which the C–H bonds in methane, ethylene, and acetylene are activated in eq 1.

Some of the reactions mentioned here have been investigated before by theoretical methods.[7] However, this is the first comprehensive study in which the whole series of reactions in eq 1 are examined by the same theoretical scheme. The present investigation models in addition the actual Cp^*_2Sc-R systems by Cp_2Sc-R rather than Cl_2Sc-R or H_2Sc-R.

All calculations are based on approximate density functional theory[10,11] which over the past decade has emerged as a tangible and versatile computational method. It has been employed successfully to obtain thermochemical data;[11,12] molecular structures;[13,14] force fields and frequencies;[15] assignments of NMR,[16,17] photoelectron,[18] ESR,[19] and UV spectra;[15] transition state structures as well as activation barriers;[20] dipole moments;[21] and other one-electron properties. Thus, approximate DFT is now applied to many problems previously covered exclusively by ab initio Hartree–Fock (HF) and post-HF methods. The recently acquired popularity of approximate DFT stems in large measure from its computational expedience which makes it amenable even to large size molecules at a fraction of the time required for HF or post-HF calculations. More importantly, perhaps, is the fact that expectation values derived from approximate DFT in most cases are better in line with experiment than results obtained from HF calculations. This is in particular the case for systems involving transition metals. As analysis of why approximate DFT affords more reliable results than HF has recently been published by Cook and Karplus[22] as well as Tschinke and Ziegler.[23] All reported equilibrium structures were confirmed to represent energy minima by considering the force constant matrix over the optimization variables.

II. Computational Details

The reported calculations were all carried out by utilizing the HFS–LCAO program system A–MOL, developed by Baerends et al.[24,25] and vectorized by Ravenek.[25b] The numerical integration procedure applied for the calculations was developed by Boerrigter[26] et al. All molecular structures were optimized on the singlet energy surface within the C_s symmetry group. The geometry optimization procedure was based on the method developed by Versluis and Ziegler.[13] Vibrational frequencies were evaluated from force constants calculated by numerical differentiation of the energy gradients.[15] The transition state was optimized according to the method of Simons et al.[27] in the implementation by Baker[28] which has been adopted to the HFS-LCAO program system by Fan.[15] The electronic configurations of the molecular systems were described by an uncontracted triple-ζ STO basis set[29] on scandium for 3d, 4s, and 4p as well as a double-ζ STO basis set[29] on carbon (2s, 2p) and hydrogen (1s). Hydrogens and carbons not on the Cp rings were given an extra polarization function: $3d_C$ (ζ_{3d} = 2.0); $2p_H$ (δ_{2p} = 2.0). The $1s^22s^22p^6$ configuration on scandium and the $1s^2$ configuration on carbon were assigned to the core and treated by the frozen-core approximation.[24] A set of auxiliary[30] s, p, d, f, and g STO functions, centered on all nuclei, was used in order to fit the molecular density and present Coulomb and exchange potentials accurately in each SCF cycle. Energy differences were calculated by including the local exchange-correlation potential by Vosko[31a] et al. with Becke's[31b] nonlocal exchange corrections and Perdew's[31c] nonlocal correlation correction. Geometries were optimized without including nonlocal corrections. The influence of nonlocal corrections on geometries has been shown[32f] to be modest. The application of approximate density functional theory to organometallic chemistry has been reviewed recently.[10c,32] The average CPU time on an IBM-6000/320 machine required in one geometry cycle was 30 min for the Cp_2Sc-R systems.

III. Hydride, Alkyl, Alkenyl, and Alkynyl Derivatives of Scandocene. Their Structures and Stability

The Cp_2Sc-R molecules, **1**, have been isolated and studied by Thompson[3b] et al. for R = H, CH_3, CH_2CH_3, and $CH_2CH_2CH_3$.

(10) (a) Parr, R. G.; Yang, W. In *Density-Functional Theory of Atoms and Molecules*; Oxford University Press: New York, 1989. (b) Kryachko, E. S.; Ludena, E. V. *Density Functional Theory of Many Electron Systems*; Kluwer Press: Dordrecht, 1991. (c) Ziegler, T. *Chem. Rev.* **1991**, *91*, 651.
(11) Becke, A. D. *Int. J. Quantum Chem.* **1989**, *S23*, 599.
(12) (a) Ziegler, T.; Tschinke, V.; Versluis, L.; Baerends, E. J.; Ravenek, W. *Polyhedron* **1988**, *7*, 1625.
(13) Versluis, L.; Ziegler, T. *J. Chem. Phys.* **1988**, *88*, 322.
(14) Fournier, R.; Andzelm, J.; Salahub, D. R. *J. Chem. Phys.* **1989**, *90*, 6371.
(15) Fan, L.; Versluis, L.; Ziegler, T.; Baerends, E. J.; Ravenek, W. *Int. J. Quantum Chem.* **1988**, *S22*, 173.
(16) (a) Bieger, W.; Seifert, G.; Eschrig, H.; Grossman, G. *Chem. Phys. Lett.* **1985**, *115*, 275. (b) Freier, D. A.; Fenske, R. F.; Xiao-Zeng, Y. *J. Chem. Phys.* **1985**, *83*, 3526. (c) Malkin, V. G.; Zhidomirov, Z. *Zh. Strukt. Khim.* **1988**, *29*, 32.
(17) van der Est, A. J.; Barker, P. B.; Burnell, E. E.; de Lange, C. A.; Snijders, J. G. *Mol. Phys.* **1985**, *56*, 1.
(18) Case, D. A. *Annu. Rev. Phys. Chem.* **1982**, *33*, 151.
(19) (a) Noodleman, L.; Norman, J. G. *J. Chem. Phys.* **1979**, *70*, 4903. (b) Noodleman, L. *J. Chem. Phys.* **1981**, *74*, 5737. (c) Noodleman, L.; Baerends, E. J. *J. Am. Chem. Soc.* **1984**, *106*, 2316. (d) Noodleman, L.; Norman, J. G.; Osborne, J. H.; Aizman, A.; Case, D. A. *J. Am. Chem. Soc.* **1985**, *107*, 3418.
(20) Fan, L.; Ziegler, T. *J. Chem. Phys.* **1990**, *92*, 3645.
(21) Trsic, M.; Ziegler, T.; Laidlaw, W. G. *Chem. Phys.* **1976**, *15*, 383.
(22) Cook, M.; Karplus, M. *J. Phys. Chem.* **1987**, *91*, 31.
(23) Tschinke, V.; Ziegler, T. *J. Chem. Phys.* **1990**, *93*, 8051.
(24) Baerends, E. J.; Ellis, D. E.; Ros, P. *Chem. Phys.* **1973**, *2*, 41.
(25) (a) Baerends, E. J. Ph.D. Thesis, Vrije Universiteit, Amsterdam, 1975. (b) Ravenek, W. In *Algorithms and Applications on Vector and Parallel Computers*; te Riele, H. J. J., Dekker, Th. J., van de Vorst, H. A., Eds.; Elsevier: Amsterdam, 1987.
(26) Boerrigter, P. M.; te Velde, G.; Baerends, E. J. *Int. J. Quantum Chem.* **1988**, *33*, 87.
(27) Simons, J.; Jorgensen, P.; Taylor, H.; Ozment, J. *J. Phys. Chem.* **1983**, *87*, 2745.
(28) Baker, J. *J. Comput. Chem.* **1986**, *7*, 385.
(29) (a) Snijders, G. J.; Baerends, E. J.; Vernooijs, P. *At. Nucl. Data Tables* **1982**, *26*, 483. (b) Vernooijs, P.; Snijders, G. J.; Baerends, E. J. Slater Type Basis Functions for the Whole Periodic System. Internal Report; Free University of Amsterdam: The Netherlands, 1981.
(30) Krijn, J.; Baerends, E. J. Fit Functions in the HFS-Method. Internal Report (in Dutch); Free University of Amsterdam: The Netherlands, 1984.
(31) (a) Vosko, S. H.; Wilk, L.; Nusair, M. *Can. J. Phys.* **1990**, *58*, 1200. (b) Becke, A. D. *Phys. Rev.* **1988**, *A38*, 2398. (c) Perdew, J. P. *Phys. Rev.* **1986**, *B33*, 8822.
(32) (a) Ziegler, T. *J. Pure Appl. Chem.* **1991**, *63*, 873. (b) Ziegler, T.; Versluis, L. *Adv. Chem. Res.* **1991**, *91*, 651. (c) Ziegler, T.; Tschinke, T. *ACS Symp. Ser.* **1990**, *No. 428*, 277. (d) Ziegler, T.; Snijders, J. G.; Baerends, E. J. *ACS Symp. Ser.* **1989**, *No. 383*, 322. (e) Ziegler, T.; Tschinke, V.; Versluis, L. *NATO ASI Ser.* **1986**, *C176*, 189. (F) Fan, L.; Ziegler, T. *J. Chem. Phys.* **1991**, *95*, 7401.

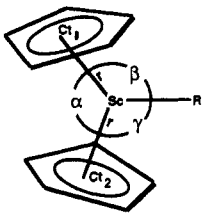

1

We have optimized Cp_2Sc-H, **2a**, and Sp_2Sc-CH_3, **2b**, under C_s symmetry constraints. In these and the following optimizations involving the Cp_2Sc fragment, only r and α of the Cp_2Sc framework, **1**, were optimized. Here r is the distance from Sc to either of the Cp centroids, Ct_1 or Ct_2, and α is the $Ct_1-Sc-Ct_2$ angle.

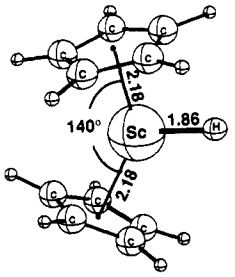

2a

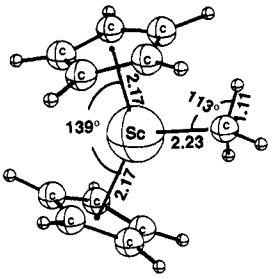

2b

We can compare our optimized structure for Cp_2Sc-CH_3, **2b**, with that determined experimentally by Thompson et al.[3b] for the methylated analogue, $Cp^*_2Sc-CH_3$ ($Cp^* = \eta^5-C_5H_5$). The structural parameters by Thompson et al.[3b] of $\alpha = 144°$, $r = 1.17$ Å, and Sc–C(Me) = 2.24 Å are in excellent agreement with our findings for Cp_2Sc-CH_3, **2b**. Our optimized structure revealed a methyl group with an approximate C_3 axis and three equivalent C–H bonds of normal length, 1.11 Å. Further, the three Sc–H distances in **2b** of 2.87 Å are much longer than the scandium–hydrogen bond length of 1.86 Å in the scandocene hydride **2a**. The long Sc–H distances in **2b** are not indicative of any interaction between the methyl hydrogens and the scandium center. In a number of cases, electron-rich C–H bonds can act as donors toward electron-poor early transition metals. Such interactions have been called agostic.[33] Methyl groups involved in agostic interactions exhibit elongated C–H bonds (1.15 Å to 1.21 Å) and a distortion, **2c**, of the tetrahedral coordination around carbon,[2]

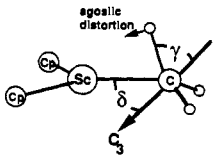

2c

with γ of **2c** larger than 109°. We have attempted optimizations of Cp_2Sc-CH_3 starting from a structure in which the C_3 axis made an angle δ, **2c**, with the Sc–C bond vector and one hydrogen was distorted away from the C_3 axis toward scandium with $\gamma > 109°$. Optimizations starting from different values of δ and γ converged in all cases back to the unperturbed methyl structure, **2b**. Thompson et al.[3b] were not able to locate the methyl hydrogens in $Cp^*_2Sc-CH_3$. However, their NMR and IR spectra are consistent with an unperturbed methyl as in **2b**. There has been several experimental[33] and theoretical[34] studies on possible agostic interactions in methyl complexes of early transition metals, L_nM-CH_3.

(33) Brookhart, M.; Green, M. L. M. *J. Organomet. Chem.* **1983**, *250*, 395.

(34) (a) Williamson, R. L.; Hall, M. B. *ACS Symp. Ser.* **1989**, *No. 394*, 17. (b) Rösch, N.; Knappe, P. *ACS Symp. Ser.* **1989**, *No. 394*, 37. (c) Koga, N.; Morokuma, K. *ACS Symp. Ser.* **1989**, *No. 394*, 77.

Table I. H–R Bond Energies[i]

		bond dissociation energies			
		exptl		calcd	
molecule	bond	D_e	D_0	D_e	D_0
H_2	H–H	463[a]	432[a]	472	441
CH_4	C–H	468[c]	431[b]	469	435
C_2H_6	C–H		416[d]	451	414
C_3H_8	C–H[e]			440	
C_2H_5	C_β–H[f]			179	
C_2H_4	C–H		459[b]	486	451
C_2H_2	C–H		549[b]	586	555
$CH_3CH_2CH_2$	$C_\gamma-C_\beta$[g]			120	
$CHCH_2$	C_β–H[h]			193	

[a] Reference 37a. [b] Reference 37b. [c] Reference 42. [d] Reference 40e. [e] C–H bond energy in propane for terminal carbon. [f] C–H bond energy in ethyl radical for β-carbon. [g] $CH_3-CH_2CH_2$ bond energy in propyl radical. [h] C–H bond in vinyl radical for β-carbon. [i] All energies in kJ mol^{-1}.

Table II. Sc–R Bond Energies[c]

molecule	bond	bond dissociation energy D_e (calcd)
Cp_2Sc-H	Sc–H	340
Cp_2Sc-CH_3	$Sc-CH_3$	295
$Cp_2Sc-C_2H_5$[a]	$Sc-C_2H_5$	283
$Cp_2Sc-C_3H_7$[b]	$Sc-C_3H_7$	240
$Cp_2Sc-C_2H_3$	$Sc-C_2H_3$	338
$CpSc-C_2H$	$Sc-C_2H$	540

[a] With respect to **3a**. [b] With respect to **4b**. [c] All energies in kJ mol^{-1}.

An agostic distortion carried to the extreme will result in a hydrido carbene complex. It was not possible to locate an energy minimum representing a hydrido carbene complex, $Cp_2Sc(H)CH_2$. Starting from suitable initial structures of the hydrido carbene complex, unrestrained optimizations on $Cp_2Sc(H)CH_2$ resulted inadvertently in the methyl complex **2b**. However, a constrained optimization in which one Sc–H bond was fixed at 1.86 Å afforded a hydrido carbene complex with an energy that is 207 kJ mol^{-1} above the methyl complex of **2b**. Our findings would indicate that the type of α-elimination given in eq 3 is unlikely to occur. Table

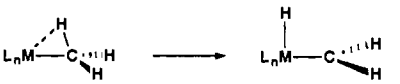

(3)

II displays calculated Sc–R bond energies for Cp_2Sc-R. We find the Sc–H bond at $D_e(Sc-H) = 340$ kJ mol^{-1} to be somewhat stronger than the $Sc-CH_3$ bond with $D_e(Sc-CH_3) = 295$ kJ mol^{-1}. The main contribution to the weaker $Sc-CH_3$ bond comes from repulsive interactions[6d] between the occupied σ_{CH} orbitals on CH_3 and the occupied core-type 3s and 3p orbitals on the metal. These types of interactions are not present in the M–H bond since hydrogen is a pure one-electron ligand.[6d] The $D_e(Sc-CH_3)$ bond energy is further reduced by 25 kJ mol^{-1} due to the relaxation of the CH_3 fragment from trigonal pyramidal in Cp_2Sc-CH_3 to planar in the methyl radical. The analogous H–R bonds are both stronger and in addition quite similar to $D_e(H-H) = 472$ kJ mol^{-1} and $D_e(H-CH_3) = 469$ kJ mol^{-1} (Table I).

Two ethyl complexes were optimized. The first one, **3a**, has a clear agostic structure with a stretched C–H bond of 1.16 Å and a Sc–H distance of 1.976 Å. The latter distance is only 0.1 Å longer than the regular Sc–H bond in the hydride complex **3a**. The C–C bond in **2a** is calculated to be 1.49 Å which is 0.05 Å shorter than a regular single C–C bond. This is understandable as **3a** in part can be viewed as a precursor for a hydrido olefin complex. The $Sc-C_\alpha-C_\beta$ angle at 82° is further seen to be slightly strained. The second structure, **3b**, is 39 kJ mol^{-1} higher in energy and represents a regular ethyl complex without agostic interactions. The $C_\alpha-C_\beta$ bond distance in **3b** is now close to a normal C–C single bond and the $Sc-C_\alpha-C_\beta$ angle nearly tetrahedral. The energy difference between **3a** and **3b** is large enough to suggest that the ethyl complex might be agostic at least at lower temperatures. Entropic factors will likely work against the more ordered con-

formation **3a** at higher temperatures. The geometrical information about the Cp_2Sc framework is omitted in **3a** and **3b** as well as in all later structures for the sake of clarity. The α angle of **1** is in general 140 ± 4° and the r distance 2.17 ± 0.02 Å.

The C–H bond in ethane has a calculated D_e(C–H) value of 451 kJ mol^{-1} which is lower than the D_e(C–H) value in methane of 469 kJ mol^{-1} (Table I). The small difference is not so much related to an inherent difference in the H–CH_3 and H–C_2H_5 bonding interactions as to the fact that the ethyl group after C–H bond dissociation is better able to stabilize the single electron by hyperconjugation. The above trend in H–R bond dissociation energies would suggest that D_e(Sc–CH_3) should be marginally larger than D_e(Sc–C_2H_5). We calculate, in fact, D_e(Sc–C_2H_5) at 283 kJ mol^{-1} to be 12 kJ mol^{-1} below D_e(Sc–CH_3) at 295 kJ mol^{-1}. However, it must be remembered that D_e(Sc–C_2H_5) is with respect to **3a**, which is stabilized by an agostic β-hydrogen interaction. Without this stabilization, as in **3b**, D_e(Sc–C_2H_5) is calculated to be 256 kJ mol^{-1}.

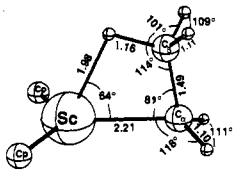

3a

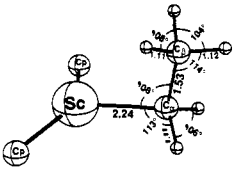

3b

The agostic hydrogen in **3a** might β-eliminate to form the hydride, **2a**, and free olefin. The reaction enthalpy, ΔH_{4a}, for the full β-elimination reaction

$$Cp_2Sc{-}C_2H_5 \rightarrow Cp_2Sc{-}H + H_2C{=}CH_2 \qquad (4a)$$

is given by

$$\Delta H_{4a} = \Delta H_e(H{-}CH_2CH_2) + \Delta H_e(Sc{-}C_2H_5) - \Delta H_e(Sc{-}H) \qquad (4b)$$

We calculate ΔH_{4a} to be 115 kJ mol^{-1}. The enthalpy ΔH_{4a} is primarily determined by the C_β–H bond energy, ΔH_e(H–CH_2CH_2), for the ethyl radical calculated at 179 kJ mol^{-1} (Table I). There is a secondary contribution from the difference ΔH_e(Sc–C_2H_5) – ΔH_e(Sc–H) which we calculate to be 64 kJ mol^{-1}. The difference ΔH_e(M–R) – ΔH_e(M–H) might be more negative for other systems if M is an electron-rich late transition metal or R a larger alkyl group. In these cases a full β-elimination should be less endothermic. Burger[3a] et al. have estimated the activation enthalpy, $\Delta H^{\ddagger}$, for β-decomposition of several Cp*Sc–R systems. They found values for $\Delta H^{\ddagger}$ close to 75 kJ mol^{-1} which is in reasonable agreement with the 115 kJ mol^{-1} calculated for ΔH_{4a}.

β-Elimination of a hydrogen from **3a** could lead to a hydrido olefin complex, **3c**, rather than the hydride, **2a**, and a free olefin. It was not possible to find an energy minimum corresponding to a hydrido olefin complex **3c**. Optimizations from various starting structures for a hydrido olefin complex converged invariably to the agostic ethyl structure, **3a**. The structure **3c** was optimized by fixing the Sc–H distance at 1.86 Å. The π-complexation energy in **3c** was calculated to be 10 kJ mol^{-1} and stems from a weak interaction between the occupied π orbital with empty metal orbitals.

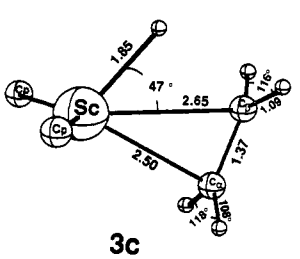

3c

The most stable conformation for the propyl derivative of scandocene was calculated to have the geometry given in **4b**. The propyl group in **4b** is almost undistorted, and only the α-carbon is interacting with the metal center. The two conformations **4c** and **4d** have virtually the same stability as **4b** with energies that

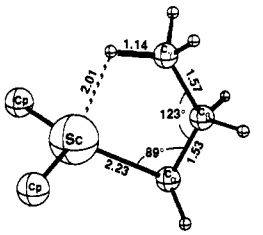

4a

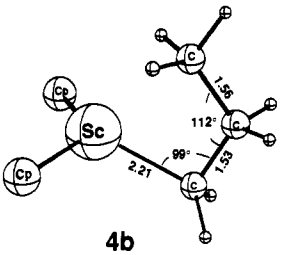

4b

are respectively 1 kJ mol^{-1} and 2 kJ mol^{-1} above **4b**. The two structures **4c** and **4d** are characterized by agostic β-hydrogen interactions. Conformation **4c** has two agostic β-hydrogens. The Sc–H distances of 2.20 Å are longer than the normal hydride bond in **2a** of 1.86 Å but still short enough to enable Sc–H interactions. The C_β–H bond distances of 1.13 Å are slightly elongated, and the Sc–C_α–C_β angle adopts a rather acute value of 72° in order to facilitate the Sc–H interactions. Conformation **4d** has a single β-hydrogen involved in an agostic interaction. The C–H_β bond is stretched to 1.17 Å and the Sc–H distance is 1.98 Å with a Sc–C_α–C_β angle of 80°.

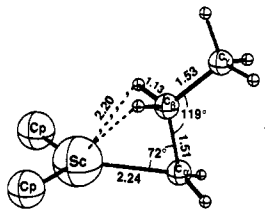

4c

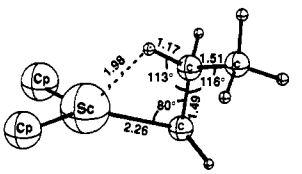

4d

The propyl group might also interact with the metal center through its γ-hydrogens. We have optimized a structure, **4a**, in which a γ-hydrogen is involved in an agostic interaction with scandium. The Sc–H and C–H_γ distances are 2.01 Å and 1.14 Å, respectively. Conformation **4a** is 29 kJ mol^{-1} above **4b** in energy. The agostic interaction between scandium and the γ-hydrogen enforces a distorted C_α–C_β–C_γ framework, and the strain from this distortion is responsible for the relatively high energy of conformation **4a**.

We calculate the Sc–propyl dissociation energy for **4b** as D_e(Sc–propyl) = 240 kJ mol^{-1} which is 14 kJ mol^{-1} below the calculated D_e(Sc–ethyl) value for **3b**. By comparison D_e(H–propyl) is calculated to be smaller than D_e(H–ethyl) by 11 kJ mol^{-1} (Table I).

Cp_2Sc–propyl can decompose by way of β-hydrogen elimination, presumably via **4d**, in a way similar to that discussed above for Cp_2Sc–ethyl. We expect the thermochemistry for the two β-hydrogen elimination processes to be quite similar. Alternatively, Cp_2Sc–propyl could decompose by a β-methyl extrusion[3d]

$$Cp_2Sc{-}CH_2CH_2CH_3 \rightarrow Cp_2Sc{-}CH_3 + H_2C{=}CH_2 \qquad (5a)$$

to produce Cp_2Sc–CH_3 and ethylene. β-Methyl extrusion has, in fact, been observed by Watson[3d] to be competitive with β-hydrogen elimination. The reaction enthalpy for (5b) is given by

$$\Delta H_{5a} = \Delta H_e(CH_3{-}CH_2CH_2) + \Delta H_e(Sc{-}C_3H_7) - \Delta H_e(Sc{-}CH_3) \qquad (5b)$$

According to our calculations (Table I), $\Delta H_e(CH_3{-}CH_2CH_2)$ = 120 kJ mol^{-1}, whereas $\Delta H_e(Sc{-}C_3H_7) - \Delta H_e(Sc{-}CH_3)$ = –55 kJ mol^{-1}. The resulting value for ΔH_{5a} is 65 kJ mol^{-1}, which is almost half of that calculated for β-hydrogen elimination in eq 4a. It follows from our considerations that β-methyl extrusion is less endothermic than β-hydrogen elimination. This is so since the C–C bond broken in β-methyl extrusion is weaker than the C–H bond broken in β-hydrogen elimination.

We have finally studied alkenyl and alkynyl derivatives of scandocene in the form of respectively the vinyl complex, **5a**, and the acetylide complex, **5b**. We find the Sc–C distances for the

sp^2 vinyl, **5a**, and the sp acetylide, **5b**, to be 2.20 Å and 2.18 Å,

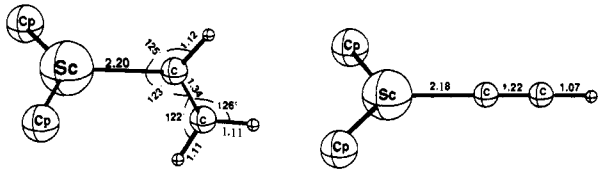

5a 5b

respectively, as compared to the Sc–C distance of 2.23 Å in the sp^3 methyl complex, **2b**. It is not surprising that the Sc–C bond becomes shorter as the role of the 2s orbital in the Sc–C bond increases. In fact, Rappé[35] finds a similar trend in his theoretical study on $Cl_2Sc–R$ (R = CH_3, C_2H_3, and C_2H). The optimized C–C distances of 1.34 Å and 1.21 Å, respectively, are quite similar to Rappé's results and point to a very small perturbation of the π-systems.

We calculate the Sc–vinyl bond with D_e(Sc–vinyl) = 338 kJ mol^{-1} to be stronger than the Sc–alkyl bonds by nearly 50 kJ mol^{-1} (Table II). An even larger increase is observed for the Sc–acetylide bond with D_e(Sc–acetylide) = 540 kJ mol^{-1} (Table II). The Sc–R bond is formed between a singly occupied σ_{Sc} orbital on Cp_2Sc of high energy and a singly occupied σ_R orbital on R of lower energy. The Sc–R bond is strongly polarized toward R, and much of its stability is due to a transfer of charge from σ_{Sc} to σ_R. The σ_R orbital of acetylide is 4 eV below σ_{Sc} and 2 eV lower in energy than the σ_R orbitals of either methyl or vinyl. The transfer of charge is as a consequence highly favorable for R = acetylide and the corresponding Sc–R bond particularly strong. The low energy of σ_R for acetylide stems from the high contribution to this orbital from 2s on carbon. For alkenyls and in particular alkyls, the 2s orbital goes into forming C–H bonds adjacent to the σ_R orbital.

Absolute Sc–R bond energies are not known experimentally. Bulls[36] et al. have measured Sc–R dissociation energies relative to the Sc–H bond strength. They find the Sc–acetylide bond to be stronger than the Sc–H linkage by more than 125 kJ mol^{-1}. On the other hand, the Sc–R alkyl bond was found to be weaker than the Sc–H linkage by 70 kJ mol^{-1} for R = $-CH_2CH_2CH_2C_6Me_4$. The calculated Sc–acetylide and Sc–alkyl bond energies given in Table II are seen to follow similar trends.

The thermodynamical considerations up to this point have all been based on the electronic bond dissociation energies, D_e, rather than D_0, which include the vibrational zero-point energy correction. D_0 value has been measured with high accuracy[37] for some of the H–R systems and we have evaluated zero-point energies for the same molecules in order to compare with experiment, Table I. The deviation between experiment and theory does not exceed 10 kJ mol^{-1} and testify to the high accuracy obtained by nonlocal DFT. The present and previous investigations[10c,38,39] confirm that nonlocal[31b,c] DFT afford bond energies of the same accuracy as the highest level of ab initio theory represented by Pople's G1[40] and G2[41] methods as well as Carter's and Goddard's CCCI scheme.[42]

(35) Rappé, A. K. *Organometallics* **1990**, *9*, 466.
(36) Bulls, A. R.; Bercaw, J. E.; Manriquez, J. M.; Thompson, M. E. *Polyhedron* **1988**, *7*, 1409.
(37) (a) Herzberg, G. *Spectra of Diaomic Molecules*; Van Nostrand Reinhold: New York, 1950. (b) Ervin, K. M.; Gronert, S.; Barlow, S. E.; Gilles, M. K.; Harrison, A. G.; Bierbaum, V. M.; DePuy, C. H.; Lineberger, W. C.; Ellison, G. B. *J. Am. Chem. Soc.* **1990**, *112*, 5750.
(38) Becke, D. A. *J. Chem. Phys.* **1992**, *96*, 2155. Presents bond energy calculations for some 50 molecules also studied by Pople et al. in refs 39 and 40.
(39) (a) Andzelm, J.; Sosa, C.; Eades, R. *J. Phys. Chem.*, in press. (b) Fitzegerald, G.; Andzelm, J. *J. Phys. Chem.* **1991**, *95*, 19531.
(40) (a) Pople, J. A.; Head-Gordon, M.; Fox, D. J.; Raghavachari, K.; Curtiss, L. A. *J. Chem. Phys.* **1989**, *90*, 5622. (b) Curtiss, L. A.; Jones, C.; Trucks, G. W.; Raghavachari, K.; Pople, J. A. *J. Chem. Phys.* **1990**, *93*, 2537. (c) Curtiss, L. A.; Pople, J. A. *J. Chem. Phys.* **1988**, *88*, 7405. (d) Curtiss, L. A.; Pople, J. A. *J. Chem. Phys.* **1989**, *91*, 2420. (e) Rusicic, B.; Berkowitz, J.; Curtiss, L. A. *J. Chem. Phys.* **1989**, *91*, 114.
(41) Curtiss, L. A.; Jones, C.; Raghavachari, K.; Trucks, G. W.; Pople, J. A. *J. Chem. Phys.* **1991**, *94*, 7221.

IV. σ-Bond Metathesis Reactions Involving $Cp_2Sc–H$ and $Cp_2Sc–CH_3$

We shall in the following section discuss the general σ-bond metathesis reaction of eq 2, where A–B represents a Sc–H or Sc–C σ-bond, whereas C–D involves H–H or C–H single bonds. This type of reactions has been studied for scandium and other electron-poor metal centers in a number of experimental[3a,b,36] and theoretical[7a,b] investigations following the pioneering work by Watson.[3c-e]

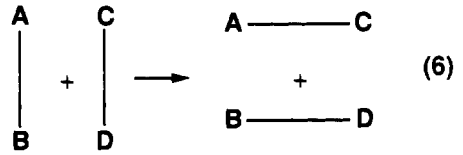

(6)

Activation of the H–H Bond. The hydrogen exchange reaction of eq 7 has been observed experimentally.[3b,4] It is exceedingly fast compared to other types of σ-bond metathesis reactions involving scandium as well as other electron-poor metals.

$$Cp_2Sc–H + D–D \rightarrow Cp_2Sc–D + H–D \quad (7)$$

Our schematic reaction profile is given in Figure 1a. We find that the degenerate metathesis process in eq 7 proceeds from reactants over a weakly bound dihydrogen adduct **6a** to the four-center transition state **6b** with a kite-shaped Sc–H–H–H core.

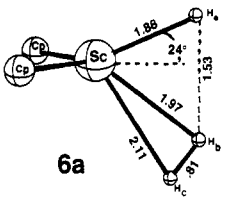

6a

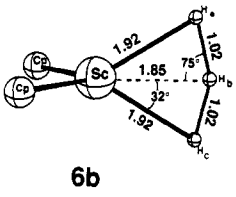

6b

The adduct formation energy for **6a** amounts to 16 kJ mol^{-1}, and the intermediate **6a** is characterized by a H–H bond which is stretched 0.04 Å compared to free H_2. The two Sc–H distances are respectively 0.11 Å and 0.25 Å, longer than the regular Sc–H bond in **2a**. Even the transition state, **6b**, is seen to be modestly more stable than the reactants by 7 kJ mol^{-1}. The kite-shaped Sc–H–H–H core in **6b** exhibits three Sc–H contacts of nearly the same lengths as the Sc–H hydride distance in **2a**, and two H–H bonds that have been stretched by 0.25 Å compared to free H_2. Thus a considerable amount of bond making and bond breaking has taken place in **6b**. On the whole, the loss in H–H interaction energy experienced by **6b** is compensated for by the formation of two new Sc–H links so that the transition state is of nearly the same energy as the reactants. It can be concluded from Figure 1a that the hydrogen exchange reaction of eq 7 will proceed readily without any barrier. In fact, the entire potential surface connecting $Cp_2Sc–H + D_2$ with Sc–D and Sc–D + HD is so shallow that substantial geometrical distortions of **6a** and **6b** can be accomplished essentially without changing the total energy. It is thus likely that individual reaction paths can proceed through structures that deviate considerably from **6a** and **6b**. The force constant matrix over the optimization variables had one negative eigenvalue for the transition state **6b**.

Steigerwald[7a] and Goddard have previously modeled the hydrogen exchange reaction of eq 7 by replacing Cp with Cl. Their optimized transition state has essentially the same geometry for the kite-shaped Sc–H–H–H core as **6b**. Steigerwald[7a] and Goddard obtained an activation energy of 71 kJ mol^{-1} (17 kcal mol^{-1}). This rather large value is not consistent with the high rates of 10^3 s^{-1} M^{-1} (−90 °C) observed[3b,4] for the hydrogen exchange reaction in eq 7. One possible reason for the discrepancy might be the use of Cl instead of Cp. However, DFT-based calculations on the chloro system afforded results quite similar to those obtained in Figure 1a. Thus with Cl as a coligand, **6a** and **6b** are 19 kJ mol^{-1} and 7 kJ mol^{-1} more stable, respectively, than the reactants $Cl_2Sc–H + H_2$.

(42) Carter, E. A.; Goddard, W. A. *J. Chem. Phys.* **1988**, *88*, 3132.

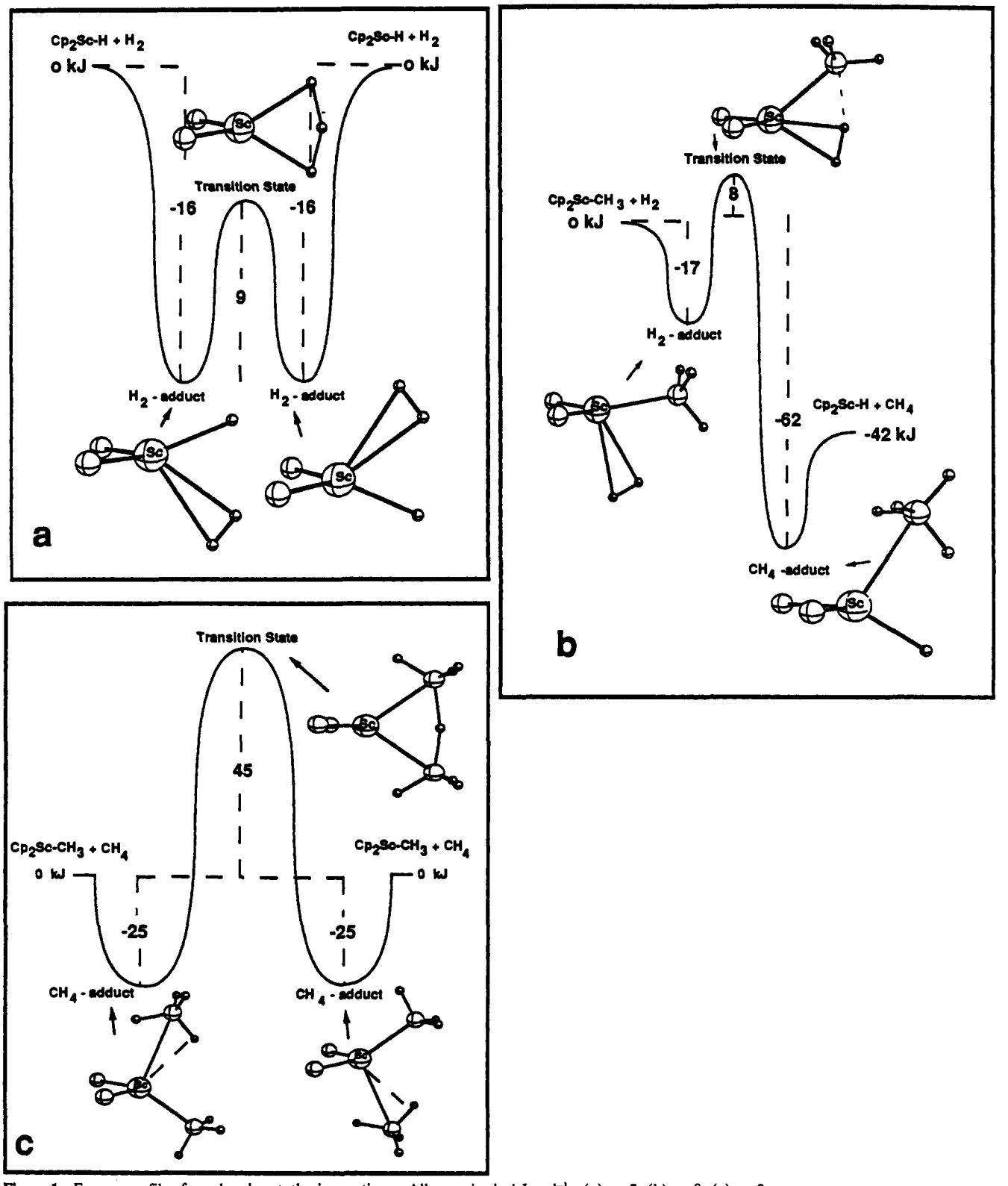

Figure 1. Energy profiles for σ-bond metathesis reactions. All energies in kJ mol^{-1}: (a) eq 7, (b) eq 8, (c) eq 9.

The activation of a H–H bond by $Cp_2Sc–CH_3$ in the reaction of eq 4 is often referred to as hydrogenolysis. This reaction has been studied extensively by Bercaw[3a,b] et al. (M = Sc) as well as Marks[3f,g] et al. (M = Th, U), Richardson[4] et al. (M = Zr^+), and Watson[3c-e] (M = Lu). It is very facile.

$$Cp_2Sc–CH_3 + H–H \rightarrow Cp_2Sc–H + H–CH_3 \qquad (8)$$

Our calculated energy profile for the hydrogenolysis reaction of eq 8 is displayed in Figure 1b. The profile passes from an initial dihydrogen adduct, **6c**, over the transition state, **6d**, to the product-like adduct between methane and $Cp_2Sc–H$, **6e**. The reaction exhibits a modest barrier of 8 kJ mol^{-1} and an exothermicity of 42 kJ mol^{-1}.

The structure of the transition state **6d** is reached early in the process and resembles closely the H_2 adduct, **6c**, with a stretched H–H bond (0.91 Å) and two close Sc–H contacts of 1.97 Å and 2.11 Å, respectively, **6d**. The transition state is destabilized relative to the reactants by the H–H stretch as well as the tilt of the local C_3 axis on the methyl group away from the Sc–C bond vector toward the direction of the incoming hydrogen,' **6d**. The tilt of

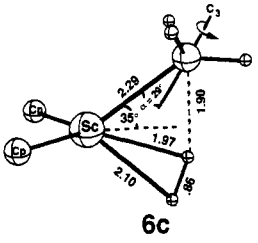

6c

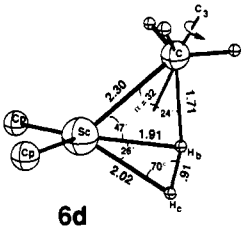

6d

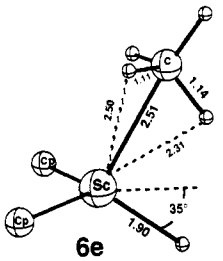

6e

the C_3 axis in **6d** by an angle α of 32° redirects the σ-orbital on CH_3 toward the incoming H-atom at the expense of losing some bonding interaction with the metal-based orbitals on scandium, thus weakening the Sc–C bond. The Sc–H_a interaction in the transition state for the hydrogen exchange reaction, **6b**, does not suffer a similar destabilization since[3b,5] the spherical nature of the $1s_a$ orbital is well suited for maintaining a strong Sc–H_a interaction, while the H_a–H_b bond to the incoming H_b atom is formed. It is thus understandable that the hydrogenolysis reaction has a lower barrier than the hydrogen exchange reaction. Several authors[3b,5] have pointed out that the 1s-hydrogen orbital is better suited to stabilize four-center transition states, **6b**, than the directional methyl σ-orbital. The small calculated barrier of 8 kJ mol^{-1} for the hydrogenolysis reaction is in harmony with experimental observations[3b] according to which the reaction is fast with a rate constant of 4×10^{-1} s^{-1} M^{-1} at −78 °C. The force constant matrix over the optimization variables of **6d** was confirmed to have one negative eigenvalue.

Activation of the Alkylic C–H Bond. The reverse of the hydrogenolysis reaction given in eq 8 represents an example where the alkylic C–H bond has been activated by Cp_2Sc–H in a σ-bond metathesis reaction:

$$Cp_2Sc\text{–}H + H\text{–}CH_3 \rightarrow Cp_2Sc\text{–}CH_3 + H\text{–}H \qquad (9)$$

It follows from our calculations that the methylation reaction in eq 9 is endothermic by 42 kJ mol^{-1} (Figure 1b). This is in line with experimental studies where Thompson[3b] et al. as well as Christ[4] et al. find that hydrogenolysis (eq 8, is more facile than methylation (eq 9), with the equilibrium in eq 9 shifted to the left. The endothermicity of eq 9 is due to the fact that a Sc–H bond is stronger than a Sc–CH_3 bond by 45 kJ mol^{-1} (Table II).

The methane exchange process

$$Cp_2Sc\text{–}C^*H_3 + H\text{–}CH_3 \rightarrow Cp_2Sc\text{–}CH_3 + H\text{–}C^*H_3 \qquad (10)$$

was discovered by Watson[3d] with lutetium as the metal atom. This process represents the first known example of methane activation by an organometallic complex. Alkyl exchange reactions have since been studied by Thompson[3b] et al. (M = Sc), Christ[4] et al. (M = Zr^+), and Marks[3f-h] et al. (M = Th, U).

The calculated energy profile for the methylation reaction is displayed in Figure 1c. The process has a barrier of 45 kJ mol^{-1} and a four-center transition state, **6g**, of C_{2v} symmetry. A methane adduct, **6f**, is formed in the early stages of the reaction with a formation energy of 25 kJ mol^{-1}. The transition state structure, **6g**, reveals that the activated C_1–H_1 bond has been stretched to 1.33 Å. The stretch is compensated for by the formation of new bonds involving C_1 as well as H_1. Thus C_1 has formed a Sc–C_1 bond with a Sc–C distances of 2.31 Å, which is only slightly longer than the Sc–C bond of 2.26 Å in **2b**. Hydrogen has at the same time established a full bond with scandium and a weaker stretched H_1–C_2 bond to the adjacent methyl carbon. The Sc–H_1 distance

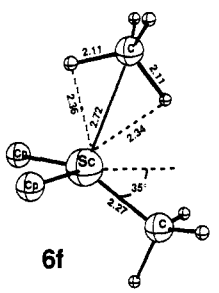

6f

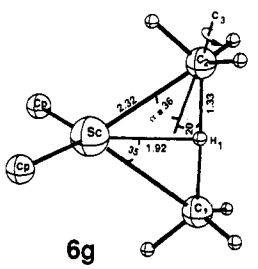

6g

of 1.92 Å is only slightly longer than the hydride distance in **2a**.

The stability of the transition state **6g** is hampered by the presence of two methyl groups in the four-center kite-shaped core. The tilt angle α in **6g** is 36° with the methyl σ-orbital directed more toward H_1 than toward the metal center. The two methyl groups have a near free rotation around their respective C_3 axis.

The C–H activation in the methyl exchange reaction, eq 10, is observed experimentally to proceed at a much slower rate than the H–H activation processes of eqs 7 and 8. Watson[43] finds an activation energy of 49 kJ mol^{-1} for the methyl exchange reaction involving lutetium which is quite close to our estimated value for the electronic barrier in the scandium system at 45 kJ mol^{-1} (Figure 1c). The force constant matrix over the optimization variables of **6g** was confirmed to have one negative eigenvalue.

We have shown that the electronic energy barrier for a σ-bond metathesis reactions increases as we increase the number of methyl groups in the kite-shaped core of the four-center transition state. We shall now discuss how vinyl and acetylide groups will influence the stability of a four-center transition state in connection with a study of σ-bond metathesis involving C–H alkenyl and alkynyl bonds.

Activation of the Alkenylic C–H Bond. Alkenes can react with L_2M–R (R = H, CH_3; L = Cp*; M = Lu, Sc, Zr^+, and Th) by insertion into the M–R bond

$$L_2M\text{—}R + H_2C\text{=}CR'R'' \rightarrow L_2M\text{—}CH_2\text{—}CRR'R'' \qquad (11)$$

or alternatively by an activation of the alkenylic C–H bond in a σ-bond metathesis reaction

$$L_2M\text{—}R + H_2C\text{=}CR'H \rightarrow L_2M\text{—}C(H)\text{=}CR'R'' + H\text{—}R \qquad (12)$$

For lutetium the simplest and least sterically hindered olefins, ethylene and propene, react by insertion,[43] whereas more bulky olefins give rise to C–H activation. For scandium[3a] only ethylene inserts into the Sc–R bond, whereas more bulky olefins than propene can insert into M–R bonds of actinides. The trend has been rationalized[3a,43] by observing that the transition state for the insertion becomes sterically crowded with more bulky olefins, in particular for the smaller sized metals such as scandium. The four-center transition state for C–H activation is sterically less demanding and thus accessible to bulkier olefins. It has further been observed that C–H activation in olefins invariably takes place at the stronger alkenylic C–H bond rather than the weaker alkylic C–H bond. We shall first discuss C–H activation (eq 12).

$$Cp_2Sc\text{—}H + H_2C\text{=}CH_2 \rightarrow Cp_2\text{—}C(H)\text{=}CH_2 + H\text{—}H \qquad (13)$$

The reaction profile for activation of a vinylic C–H bond in ethylene by Cp_2Sc–H is given in Figure 2a. The process is endothermic by 16 kJ mol^{-1} and has a modest barrier of 20 kJ mol^{-1}. The incoming ethylene forms an adduct, **7a**, which proceeds to the four-center transition state, **7b**. There is a clear resemblance between the transition states corresponding to the activation by Cp_2Sc–H of an alkylic C–H bond, **6d**, and a vinylic C–H bond, **7b**. Both structures have a largely broken C–H bond. Further,

(43) Watson, P. L. In *Selective Hydrocarbon Activation*; Davis, J. A., Watson, P. L., Liebman, J. F., Greenberg, A., Eds.; VCH Publishers: New York, 1990.

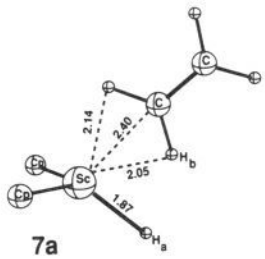

7a

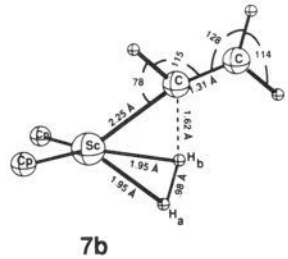

7b

the C–H bond breaking is compensated for by the formation of Sc–C and H–H bonds.

The correlation diagram for the two types of C–H activation by Cp_2Sc-H is illustrated in schematic form in Figure 3a. There are two electron pairs involved in the process. The pair of lowest energy is originally situated in a C–H σ-orbital (right-hand side of Figure 3a), which correlates smoothly with the H–H σ-orbital on the product side (left-hand side of Figure 3a). The electron pair is in the transition state extended over the α-carbon center as well as the two hydrogen atoms, with the largest amplitude on the hydrogens. The orbitals on the metal center are not involved in stabilizing the lower electron pair. The pair of highest energy resides on the reactant side in a Sc–H σ-bond which correlates on the product side with a Sc–C σ-orbital. The transition state has the upper pair situated in a three-center orbital involving d_{xy} on scandium as well as the σ_C on the α-carbon and $1s_H$ on H_a. The upper electron pair is stabilized throughout the reaction by a metal orbital which maintains optimal overlaps with the adjacent ligand orbitals by a constant rehybridization. A pool of empty s-, p-, and d-type orbitals on scandium makes such a rehybridization possible. The d_{xy} orbital is of particular importance for the stability of the electron pair in the transition state, whereas d_{xy} as well as $d_{x^2-y^2}$ play a pivotal role for the stability of the upper electron pair among the products and the reactants. The C–H bond breaking transit from **7a** to **7b** is illustrated in **7c**.

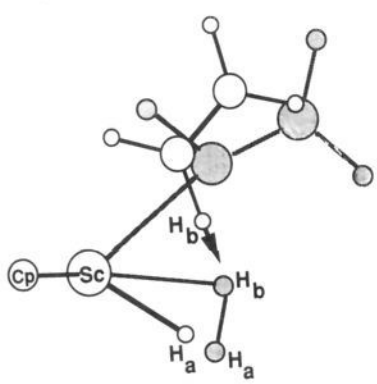

7c

The energy profile for the activation of a vinylic C–H bond by Cp_2Sc-CH_3 in eq 14 is given in Figure 2b. The reaction is

$$Cp_2Sc{-}CH_3 + H_2C{=}CH_2 \rightarrow Cp_2Sc{-}C(H){=}CH_2 + CH_4 \quad (14)$$

exothermic by 26 kJ mol^{-1} and subject to an electronic activation barrier of 39 kJ^{-1}. Thus vinylic C–H activation by Cp_2Sc-CH_3 is seen to be exothermic in contrast to corresponding process (eq 13) mediated by Cp_2Sc-H (Figure 2a). However, C–H activation by Cp_2Sc-CH_3 has a larger barrier than vinylic C–H activation involving Cp_2Sc-H.

The transition state, **8b**, exhibits a vinylic C–H bond that has been stretched to 1.34 Å as well as a methyl group for which the tilt angle α has been increased from 19° in the ethane adduct, **8a**, to 46° in the transition state. The two destabilizing factors are countered by the formation of a Sc–H bond at 1.90 Å, **8b**, as well as a vinylic Sc–C bond at 2.30 Å. The transition state for the alkylic C–H activation by Cp_2Sc-CH_3, **6g**, is in many ways similar to that, **8b**, corresponding to the vinylic C–H activation

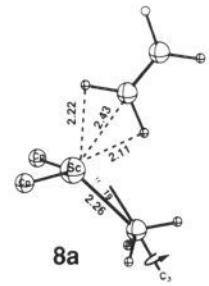

8a

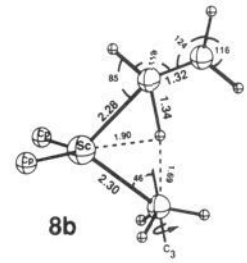

8b

by Cp_2Sc-CH_3. Both **6g** and **8b** are destabilized by the fact that the two carbon centers in the four-center core have directional σ-orbitals which are unable to sustain optimal interactions with hydrogen and the metal center at the same time. The result is a substantial electronic barrier of ~40 kJ mol^{-1}. The correlation diagram for the two types of C–H activation by Cp_2Sc-CH_3 is illustrated in schematic form in Figure 3b. The correlation diagram is very similar to that presented in Figure 3a for the corresponding C–H activation processes mediated by Cp_2Sc-H. There are again two electron pairs involved in the process, and both are stabilized by the ability of the metal center to rehybridize throughout the reaction in order to maintain overlaps with the two adjacent σ-orbitals on the carbon centers. Again, the directionality of the σ-orbitals impedes optimal simultaneous overlaps with the 1s-orbital and the metal hydrides in the two orbitals holding the active electron pairs. The energy barrier for alkenylic C–H activation by Cp^*Sc-CH_3 has been measured[3b] for *p*-methoxystyrene as 48 kJ mol^{-1}, which is not substantially different from our calculated electronic barrier of 39 kJ mol^{-1} for C–H activation in ethylene (Figure 2b). The system in **8b** was too large for a calculation of the force constant matrix, and we were thus not able to verify whether **8b** has a single negative eigenvalue.

Thompson[3b] et al. have observed that olefins containing vinylic as well as alkylic C–H bonds undergo σ-bond metathesis with Cp^*Sc-CH_3 preferably using the vinylic C–H bond. This preference could be ascribed[3b] to kinetic factors assuming that the less directional alkenylic sp^2 σ-orbital is better able to stabilize the four-center transition state than the sp^3-type alkylic σ-orbital. However, we calculate the barrier for alkenylic C–H bond activation at 39 kJ mol^{-1} (Figure 2b) to be only slightly lower than that of alkylic C–H activation at 48 kJ mol^{-1} (Figure 1c).

The preference for alkenylic C–H bond activation might alternatively be attributed to thermodynamical factors. In fact, we calculate the reaction in eq 14 to be exothermic by −26 kJ mol^{-1} which would indicate that Sc–vinyl bonds are preferred over Sc–alkyl bonds. The enthalpy for the reaction in eq 14 can be written as

$$\Delta H_{14} = [D(H{-}C_{vinyl}) - D(H{-}C_{methyl})] + [D(Sc{-}C_{methyl}) - D(Sc{-}C_{vinyl})] \quad (15)$$

The difference in the first square bracket is positive as vinylic C–H bonds are stronger than alkylic C–H bonds (Table I). Thus the first square bracket, which we calculate to be 17 kJ mol^{-1}, would favor alkylic C–H activation and shift the equilibrium to the left in eq 14. The second difference amounts to −43 kJ mol^{-1} according to our calculations (Table II). It indicates that the vinylic Sc–C bond is substantially stronger than an alkylic Sc–C bond and favors vinylic C–H activation by shifting the equilibrium to the right in eq 14. Our analysis leads to the conclusion that the preference for vinylic C–H bond activation is driven by the strength of the vinylic Sc–C bond.

We have previously calculated the reaction enthalpy for the insertion of ethylene into the Cp_2Sc-H bond as $-\Delta H_{4a} = -115$ kJ mol^{-1} (eq 4b), whereas the σ-bond metathesis reaction involving Cp_2Sc-H and ethylene (eq 13) has a reaction enthalpy of $\Delta H_{13} = 16$ kJ mol^{-1} (Figure 2a). Thus, insertion is favored over σ-bond metathesis on thermochemical grounds for the reaction between Cp_2Sc-H and ethylene. Insertion is also calculated to be favored in the reaction between Cp_2Sc-CH_3 and the ethylene molecule. Here, the reaction enthalpy for insertion is given as $-\Delta H_{5a} = -65$

kJ mol^{-1} (eq 5b), whereas σ-bond metathesis gives $\Delta H_{14} = -26$ kJ mol^{-1} (Figure 2b). We shall in a later study[44] look at the reaction profiles for insertion processes and evaluate the influence that substituents[3a,43] on either ethylene or Cp might have on the activation barrier.

Activation of the Alkynylic C–H Bond. Metal–hydride and metal–alkyl bonds of early transition metals can react[43] with alkynes via alkyne insertion (eq 16a) or C–H activation (eq 16b).

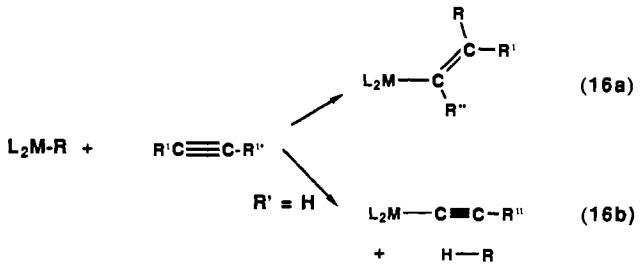

$Cp^*Sc–CH_3$ reacts exclusively[3b] with internal acetylenes to afford insertion products (eq 16a), whereas C–H activation is observed exclusively in the reaction between $Cp^*Sc–CH_3$ and terminal[3a,43] acetylenes (eq 16b). The preference observed for reactions between $Cp^*Sc–CH_3$ and alkynes indicates that this system favors alkynylic C–H activation over insertion, whereas alkylic C–H activation is less favorable than either insertion (eq 16a) or alkynylic C–H activation (eq 16b).

The activation of the C–H bond in acetylene by $Cp_2Sc–H$

$$Cp_2Sc–H + HCCH \rightarrow Cp_2Sc–CCH + H_2 \quad (17a)$$

is calculated to be strongly exothermic with a reaction enthalpy of –86 kJ mol^{-1} (Figure 2c). The reaction enthalpy can be written as

$$\Delta H_{17a} = [D_e(Sc–H) - D(Sc–CCH)] - [D_e(H–H) - D_e(H–CCH)] \quad (17b)$$

and it follows from the data in Tables I and II that the reaction in eq 17a is exothermic because the increase in strength in going from a Sc–H bond to a Sc–CCH bond is larger than the increase in going from a H–H bond to a H–CCH bond.

Acetylene forms in the early stages of the reaction a tight adduct with $Cp_2Sc–H$, **9a**, in which a C–H bond on acetylene undergoes an agostic interaction with scandium. The agostic interaction results in an elongation of the C–H bond by 0.04 Å and a short Sc–H distance of 2.07 Å, **9a**.

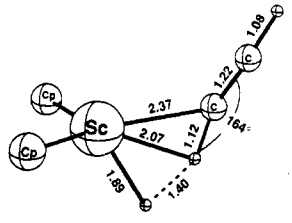

9a

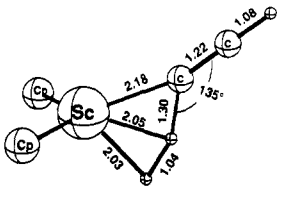

9b

The transition state, **9b**, for the process in eq 17a has the C–H bond stretched to 1.30 Å. However, this bond weakening is more than compensated for by a new H–H bond with R(H–H) = 1.04 Å and a Sc–C bond of 2.18 Å which is comparable to the Sc–C bond length of the acetylide complex, **5b**. There is in addition a close Sc–H contact of 2.06 Å. The transition state is seen to be of lower energy than the sum of the two reactants $Cp_2Sc–H$ and HCCH (Figure 2c) although slightly above (8 kJ mol^{-1}) the adduct **9a**. It is clear from Figure 2c that the activation of an alkynylic C–H bond should be a facile reaction from a thermodynamic as well as a kinetic point of view.

It might be of interest to compare the enthalpy ΔH_{17a} for the C–H activation with the enthalpy ΔH_{18a} for the alternative insertion process

$$Cp_2Sc–H + HCCH \rightarrow Cp_2Sc–C(H)CH_2 \quad (18a)$$

The enthalpy ΔH_{18a} can be written as

$$\Delta H_{18a} = [D_e(Sc–H) - D_e(Sc–C(H)CH_2)] - D_e(H–C(H)CH) \quad (18b)$$

The difference from the first two terms in eq 18b amounts to 2 kJ mol^{-1} as the Sc–H and Sc–C(H)CH_2 bonds are of nearly the same strength (Table II), whereas $-D_e$(H–C(H)CH) = –193 kJ mol^{-1} (Table I). Thus insertion has an enthalpy of $\Delta H_{18a} = -191$ kJ mol^{-1}. The favorable reaction enthalpy stems primarily from the net formation of an additional σ-bond. It follows from our estimates in eqs 17b and 18b that insertion should be favored over C–H activations on thermodynamical grounds in reactions involving scandium, and we expect the same to be true for other early transition metals. Zirconium[3i] and hafnium[3i] do, in fact, favor insertion, whereas both reactions are feasible with lutetium.[3d] For scandium,[3b] only C–H activation is observed.

Rappé has discussed the reactions in eqs 17a and 18a for a model system[8] in which the Cp rings were replaced by Cl atoms. Rappé found C–H activation to be exothermic by 63 kJ mol^{-1}, and his optimized transition state has a four-center core with a geometry very similar to that of **9b**. The transition state in Rappé's calculation was found to be 25 kJ mol^{-1} above the reactants. Thus, both sets of theoretical studies point to the activation of an alkynylic C–H bond by hydrides of early transition metals as facile. However, Rappé finds in agreement with the present investigation, and counter to experimental observation,[3b] that insertion, eq 18a, is more favorable than C–H activation with the reaction enthalpy for insertion calculated at –153 kJ mol^{-1}. It has been suggested by Rappé and others[43] that the absence of insertion must be attributed to kinetic factors. We intend to explore this point in a later study.[44]

The profile for the corresponding activation of an alkynylic C–H bond by $Cp_2Sc–CH_3$

$$Cp_2Sc–CH_3 + HCCH \rightarrow Cp_2Sc–CCH + CH_4 \quad (19)$$

is displayed in Figure 2d. At the start of the reaction, we encounter again an acetylene adduct, **10a**, where the C–H bond, which is going to be activated, is engaged in an agostic interaction with the electropositive metal center and stretched to 1.13 Å. The adduct stabilization energy is –18 kJ mol^{-1}. The activated acetylic

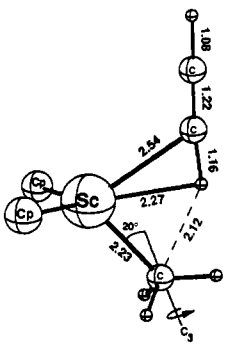

10a

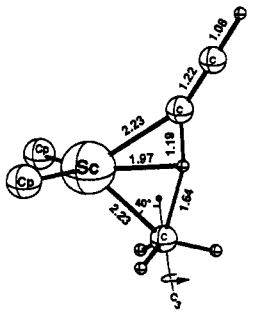

10b

C–H bond is still retained in the transition state, **10b**, although considerably weakened and stretched to 1.19 Å. The destabilization of the acetylic C–H bond is compensated for by the formation of Sc–H and Sc–C bonds at 1.97 Å and 2.23 Å, respectively. The stabilizing interaction between the electropositive scandium and the two centers on the acetylic C–H bond is primarily due to a donation of charge from the C–H bond to empty

(44) Ziegler, T.; Folga, E. Work in progress.

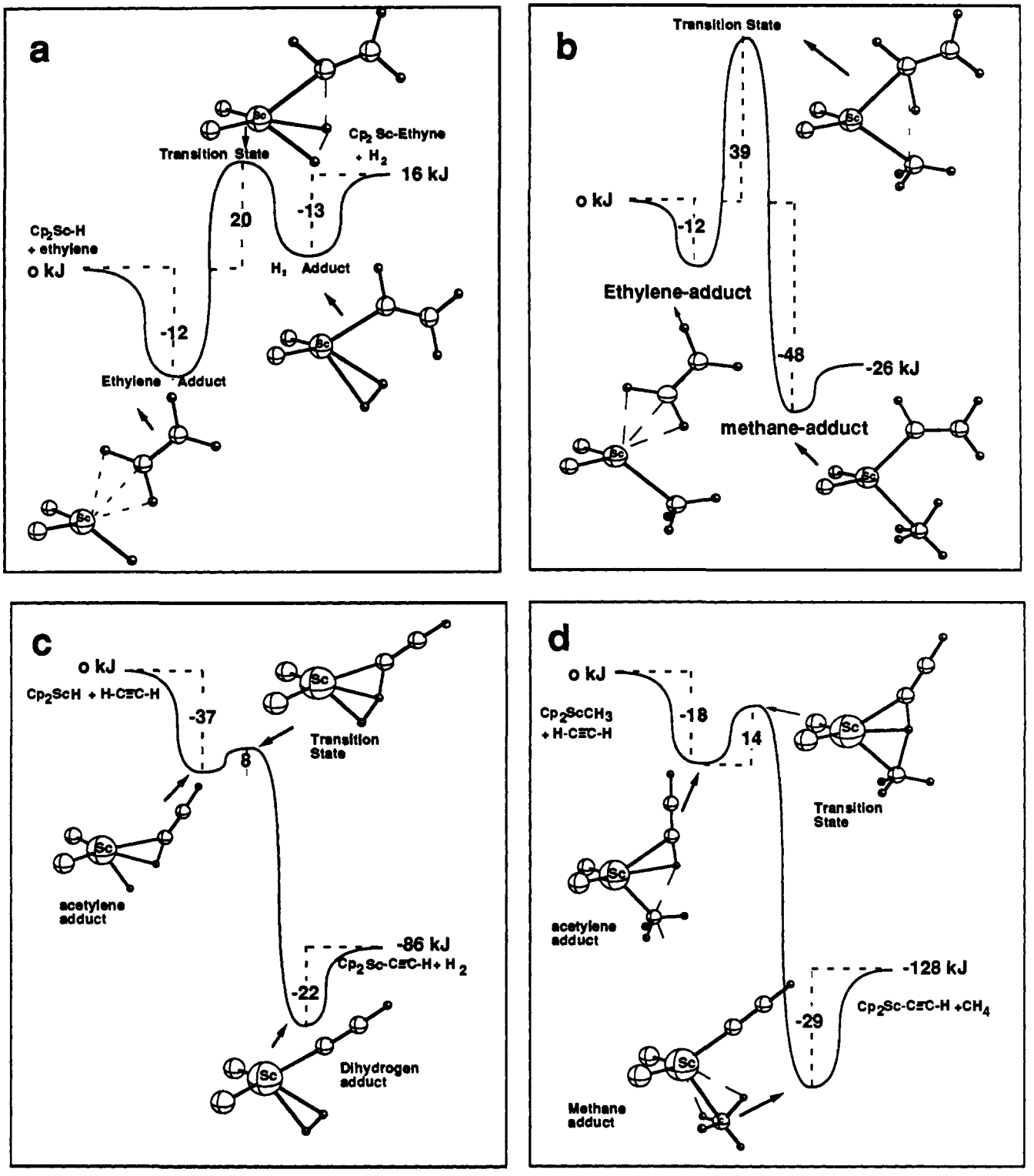

Figure 2. Energy profiles for σ-bond metathesis reactions. All energies in kJ mol^{-1}: (a) eq 13, (b) eq 14, (c) eq 17a, (d) eq 19.

orbitals on the metal. The transition state is 4 kJ mol^{-1} below the reactants in energy (Figure 2d) but still 14 kJ mol^{-1} above the acetylene adduct, **10a**. We were not able to verify whether **10b** has a single force constant matrix with a single negative eigenvalue due to the size of the system.

The C–H activation process in eq 14 is strongly exothermic with a calculated reaction enthalpy of −128 kJ/mol (Figure 2d). It is thus clear that the process is feasible from a kinetic as well as a thermodynamic point of view. In eq 19 a C–H methyl bond is formed at the expense of breaking a C–H acetylene bond which is energetically unfavorable (Table I). However, this loss in stability is more than compensated for by exchanging a Sc–methyl bond by a Sc–acetyl bond (Table II).

V. Concluding Remarks

We have studied various hydrocarbyl derivatives of scandocene. Most of the systems were found to possess a ground-state structure in which the hydrocarbyl group is bound exclusively to scandium through a single carbon atom. The only exception was the ethyl derivative in which the Sc–C bond is supplemented by an agostic interaction between the metal and a β-hydrogen. The strength of the Sc–R bonds follow the expected trend alkynyl $\gg$ alkenyl $>$ alkyl, whereas the trend in bond strength among the alkyl species

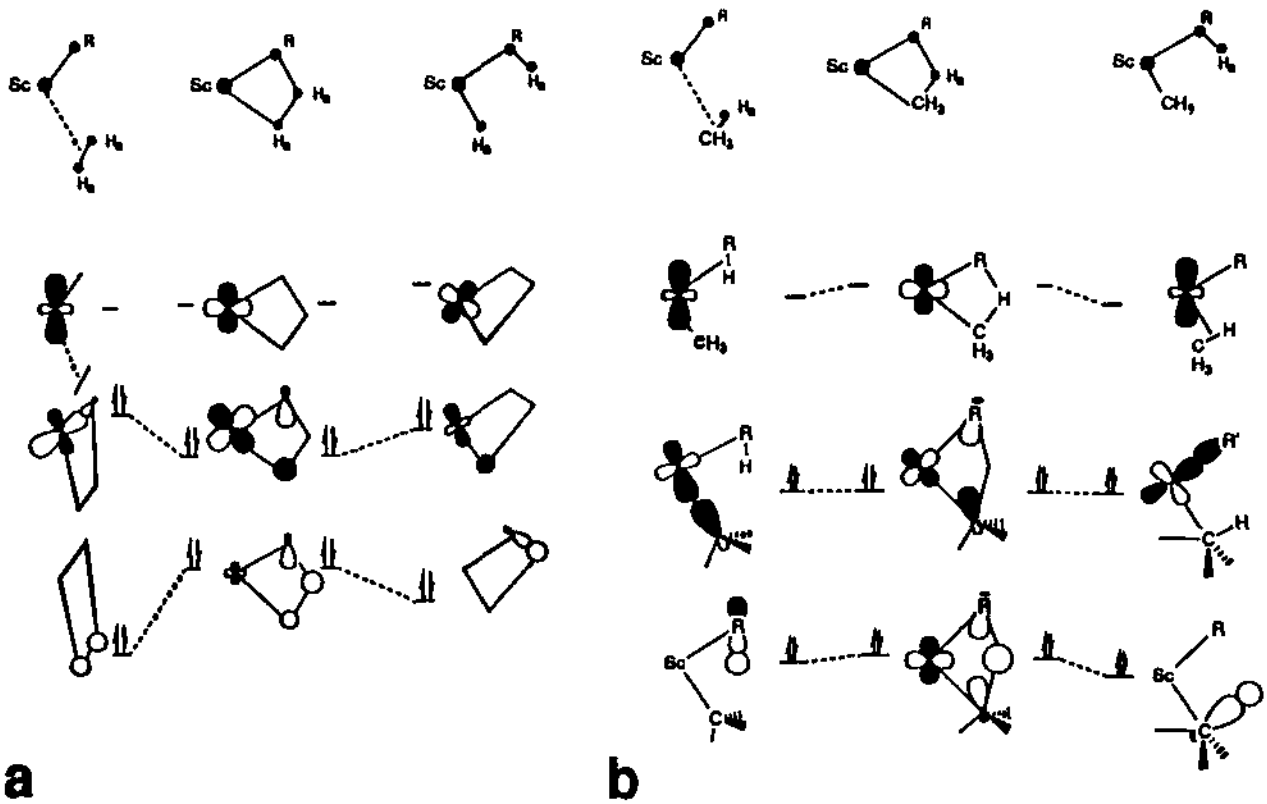

Figure 3. Schematic correlation diagrams for σ-bond metathesis reactions: (a) $Cp_2Sc-H + H-R \rightarrow Cp_2Sc-R + H_2$; (b) $Cp_2Sc-CH_3 + H-R \rightarrow Cp_2Sc-R + CH_4$ (R = alkyl and vinyl).

is methyl > ethyl > propyl. The calculated order is roughly the same as for the C–H bond in the corresponding H–R systems. We expect the calculated electronic bond dissociation energies to be accurate to within 30 kJ mol^{-1} and likely on the high side. Zero-point energy corrections are not considered here for the Sc–R bonds. They should reduce the bond energies by 10 kJ mol^{-1}. The calculated order for the bond dissociation energies conforms to the few trends observed experimentally.[36]

The second part of the study was concerned with the σ-bond metathesis reaction of eq 2. The reaction was found to involve a four center transition state. The highest activation energies, ~40 kJ mol^{-1}, were obtained in the cases where two of the four groups in the core of the kite-shaped transition state structure, I, are alkyl or alkenyl, whereas the presence of a single alkenyl or alkyl group gives rise to a somewhat lower activation energy of 10 kJ mol^{-1}. Processes involving only hydrides and alkynyl were found to have negative activation energies. The derived trends in activation energies follow closely the order in rates obtained experimentally,[3,43] and the increase in activation energy with alkyl or alkenyl groups can be understood, as suggested previously,[3b,5] from the directional nature of the σ-orbital on these groups which makes it impossible to maintain optimal interactions with both neighbors in the Sc–R–H–R′ core. It is shown that the formally forbidden [$2_\sigma + 2_\sigma$[reaction of eq 2 is made feasible by a pool of empty s-, p-, and d-type orbitals on scandium which can supply suitable hybrids appropriate for optimal interaction with the neighboring groups in the Sc–R–H–R′ core throughout the reaction.

Our calculations indicate that insertion of ethylene (eqs 4a and 5a), or acetylene (eq 18a) into the Sc–H and Sc–CH_3 bonds are preferred thermodynamically over the alternative alkenylic (eqs 13 and 14) or alkynylic (eqs 17a and 19) C–H bond activations. This is in line with experiment for ethylene.[3b] However, acetylenes have been observed[3b] to prefer alkynylic C–H activation over insertion for scandium. We expect to investigate this point further by a full study[44] in which profiles for the insertion processes of olefins and acetylenes into the L_2Sc-R bonds (R = H, alkyl) are traced for L = Cp as well as methylated derivatives of Cp.

Acknowledgment. This investigation was supported by the Natural Sciences and Engineering Research Council of Canada (NSERC). We thank Professor E. J. Baerends and Professor W. Ravenek for a copy of their vectorized LCAO–HFS program system and Dr. V. Tschinke (CIBA-Geigy, Basel) for many useful discussions. Access to the IBM-6000 computing facilities at the University of Calgary is acknowledged.